

On geometry effects in Rayleigh-Bénard convection

Siegfried Grossmann¹ and Detlef Lohse²

¹ *Department of Physics, University of Marburg, Renthof 6, D-35032 Marburg, Germany*

² *Department of Applied Physics, University of Twente, 7500 AE Enschede, Netherlands*
(March 30, 2022)

Various recent experiments hint at a geometry dependence of scaling relations in Rayleigh-Bénard convection. Aspect ratio and shape dependences have been found. In this paper a mechanism is offered which can account for such dependences. It is based on Prandtl's theory for laminar boundary layers and on the conservation of volume flux of the large scale wind. The mechanism implies the possibility of different thicknesses of the kinetic boundary layers at the sidewalls and the top/bottom plates, just as experimentally found by Qiu and Xia (Phys. Rev. E58, 486 (1998)), and also different Ra -scaling of the wind measured over the plates and at the sidewalls. In the second part of the paper a scaling argument for the velocity and temperature fluctuations in the bulk is developed.

Turbulent Rayleigh-Bénard convection is one of the classical problems in fluid dynamics [1–3]. The great interest into this problem presumably also originates from the relevance of thermal turbulence in meteorology, geophysics, oceanography, and astrophysics. However, in contrast to these natural problems, in laboratory experiments the thermal convection is confined to a container. Recent experiments have revealed that geometrical details of this container are important. Daya and Ecke [4] find that the bulk temperature and velocity fluctuations in a cylindrical cell and in a square cell are very different from each other. For cylindrical cells the aspect ratio dependence has been examined by the Ahlers group [5,6] and by the Tong group [7]; in those experiments only the prefactors of effective power laws seem to change. Niemela and Sreenivasan [8] find an aspect ratio dependence of the heat flow at large Rayleigh numbers, and conclude that the focus of the next generation of experiments must be on large aspect ratio cells.

Another recent surprising result to be mentioned in this context is the dependence of the kinetic boundary layer (BL) thickness (which is set by the mean flow velocity profile above the wall) on its location in the cell. Qiu and Xia [9,10] find that it scales differently at the sidewalls and at the top or bottom plates. They find $\delta_w/L = 3.6 Ra^{-0.26 \pm 0.03}$ for the sidewall BL thickness (from now on abbreviated with w , for wall) and $\delta_p/L = 0.65 Ra^{-0.16 \pm 0.02} Pr^{0.24 \pm 0.01}$ for the thickness at the top or bottom plates (from now on abbreviated with p , for plate), both for an aspect ratio $\Gamma = 1$ cylindrical cell. No existing theory of Rayleigh-Bénard convection accounts for this difference. Our own unifying theory of thermal convection [11,12] so far allows only for *one* kinetic

boundary layer thickness, and gives a power law exponent -0.22 (for $\Gamma = 1$ and a Prandtl number of $Pr = 6$) [12], close to the average $(-0.16 - 0.26)/2 = -0.21$ of the experimental results for the plate and the wall BL thicknesses.

In this paper we set out to offer a mechanism to account for the shape and aspect ratio dependence in Rayleigh-Bénard convection, and for the difference between the wall and plate kinetic BLs. The starting point is Prandtl's BL theory [13–15]. The main physical ingredient is the conservation of the volume flux of the large scale wind. In the second part of the paper we present scaling arguments for the fluctuations of the velocity and the temperature in the bulk.

Laminar BL flow is described by the famous Prandtl equations [13–15]. In these equations streamwise lengths are scaled by the streamwise length scale l , while wall-normal lengths are (re)scaled by l/\sqrt{Re} . Here, $Re = lU_0/\nu$ is the Reynolds number based on the streamwise length scale l and the streamwise velocity scale U_0 . Correspondingly, streamwise velocities are scaled by U_0 and wall-normal velocities by U_0/\sqrt{Re} . The immediate consequence is that the thickness of the laminar BL scales as $\delta \sim l/\sqrt{Re}$ ([13]; see also e.g. section 39 of ref. [15]).

In the context of Rayleigh-Bénard convection this means that the relevant streamwise length scales are the width d of the cell for the plates and the height L of the cell for the walls, i.e., *different* for cells with non-unity aspect ratio $\Gamma = d/L$. Correspondingly, according to the Prandtl theory, also the widths of the BLs at the walls and at the plates are different, namely,

$$\delta_w = a \frac{L}{\sqrt{U_w L/\nu}} \quad (1)$$

and

$$\delta_p = a \frac{d}{\sqrt{U_p d/\nu}}, \quad (2)$$

respectively. Here, a is a dimensionless prefactor of order 1; Blasius [14] gave $a = 1.72$ for a semi-infinite kinetic BL, cf. also [15]. If we assumed that the streamwise wall and plate velocities are the same, $U_w = U_p$, we would immediately get aspect ratio dependent BL widths $\delta_w = \delta_p/\sqrt{\Gamma}$.

However, the experiments by Tong's group [7] show that the assumption $U_w = U_p$ does not hold. Indeed, a more realistic assumption seems to us *volume flux conservation*, i.e., equal volume fluxes of the wind over the walls and the plates,

$$\dot{V}_w = \dot{V}_p. \quad (3)$$

Then the geometry of the cell immediately enters. We will discuss two extreme situations: The “confined” flow, and the “unconfined” flow, see figure 1. In the confined flow the convection roll has the *same* spanwise extension both at the plates and the walls. In contrast, the unconfined flow makes use of the full plate width d in the middle, whereas towards the walls its extension is of order $2\sqrt{d\delta_w}$ [16]. The real flow will presumably be in between these two extremes.

Confined flow: The spanwise length scale of the flow is of order $2\sqrt{d\delta_w}$ at the walls and at the plates (see figure 1). The corresponding volume fluxes are $\dot{V}_w = 2\sqrt{d\delta_w}\delta_w U_w$ at the walls and $\dot{V}_p = 2\sqrt{d\delta_w}\delta_p U_p$ at the plates. With volume flux conservation eq. (3) and the Prandtl relations (1) and (2) we immediately get

$$\delta_w/\delta_p = \Gamma^{-1}, \quad (4)$$

$$U_p/U_w = \Gamma^{-1}. \quad (5)$$

Thus the wall and plate BLs have different thicknesses. But there is *no* difference in the Ra -scaling of δ_w and δ_p , in contrast to what was found by Xia’s group [9].

Unconfined flow: The spanwise length scale of the flow at the cylindrical walls still is $2\sqrt{d\delta_w}$. But now by definition the flow at the plates is unconfined spanwise and the respective spanwise extension is of order d . The corresponding volume fluxes are now $\dot{V}_w = 2\sqrt{d\delta_w}\delta_w U_w$ at the wall and $\dot{V}_p = d\delta_p U_p$ at the plate. With volume flux conservation eq. (3) and the Prandtl relations (1) and (2) we now obtain $U_p^2/U_w = \nu L^{-1}\Gamma^{-4}2^4 a^4$ and

$$\delta_w/\delta_p = \Gamma^{-1/2}\sqrt{U_p/U_w}. \quad (6)$$

We now introduce wall and plate Reynolds numbers,

$$Re_w = U_w L/\nu, \quad Re_p = U_p L/\nu. \quad (7)$$

Note that both are defined with the height L of the cell. With these definitions we find

$$\delta_w/\delta_p = \Gamma^{-5/2}4aRe_p^{-1/2} = \sqrt{4a}\Gamma^{-3/2}Re_w^{-1/4}, \quad (8)$$

$$U_p/U_w = Re_p/Re_w = \Gamma^{-4}16a^2Re_p^{-1} = 4a\Gamma^{-2}Re_w^{-1/2}. \quad (9)$$

Equation (8) is our first main result. It shows, for unconfined flow, indeed a Reynolds number and thus a Rayleigh number dependence of the ratio between the BL thicknesses at the wall and at the plate, due to the cylindrical shape of the container. δ_w and δ_p scale differently with Ra , just as experimentally observed [9].

Since experimental flow is expected to lie in between the confined and the unconfined cases, δ_w/δ_p should be

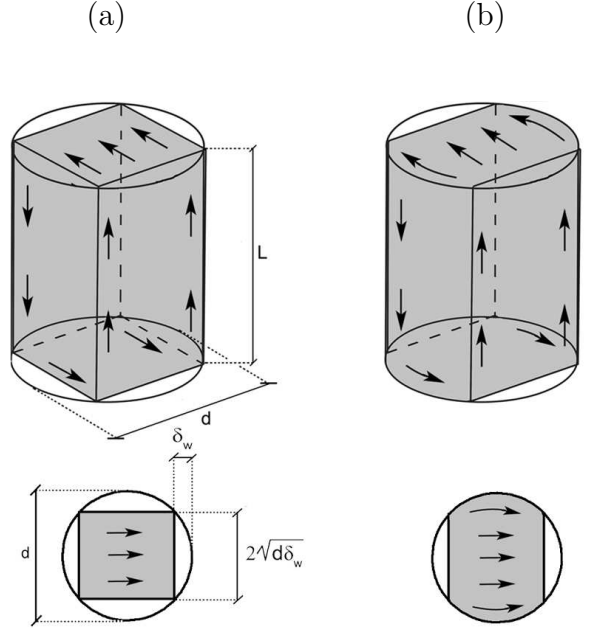


FIG. 1. Confined (a) and unconfined (b) flow in a cylindrical cell. The upper drawings show sketches of the 3D flow, the lower ones a top view on the bottom plate. The flow area above the plate is shaded. The spanwise extension of the wind along the walls is $2\sqrt{d\delta_w}$ and follows from trigonometry.

between $Re_p^{-1/2}$ and Re_p^0 or between $Ra^{-0.22}$ and Ra^0 ; here we have used the effective scaling $Re_p \sim Ra^{0.45}$ which holds for $Pr = 5$ and $\Gamma = 1$ both experimentally [7, 17] and theoretically [12] in the Ra regime $10^8 < Ra < 10^{10}$. Indeed, the experimental ratio has a scaling exponent in between the values given by the unconfined and confined cases, namely $\delta_w/\delta_p \sim Ra^{-0.11}$ [9].

We now come to our other result, eq.(9), and to the aspect ratio dependence of δ_w/δ_p and U_p/U_w . For $\Gamma = 1/2$ and $\Gamma = 2$ these ratios (as predicted in the two cases, and gauged to $\Gamma = 1$) are summarized in table I. The experimental data are obtained from figure 3 ($\Gamma = 1$, $Ra = 3.7 \cdot 10^9$), figure 6 ($\Gamma = 2$, $Ra = 4.9 \cdot 10^8$), and figure 8 ($\Gamma = 1/2$, $Ra = 3.28 \cdot 10^{10}$) of reference [7]. In this series of figures both Γ and Ra were changed at the same time. In order to compare the ratios at $\Gamma = 2$ measured at $Ra = 5 \cdot 10^8$ with those at $\Gamma = 1$ measured at $Ra = 3.7 \cdot 10^9$, they first have to be extrapolated to this higher Ra number. Correspondingly, in the $\Gamma = 1/2$ case we have to extrapolate the ratios from the original value $Ra = 3.3 \cdot 10^{10}$ to $Ra = 3.7 \cdot 10^9$. These extrapolations have been done according to the unconfined case formulas (8), (9) or according to the confined case ones (4), (5). In the latter case in fact no extrapolation is necessary as in those equations there is no Ra or Re dependence.

From table I we conclude that the experimental results (if extrapolated with the unconfined flow model) in general lie in between the predictions of the confined and unconfined cases, just as expected. An exception is

	model	$\Gamma = 1$	$\Gamma = 1/2$	$\Gamma = 2$
δ_w/δ_p	experi., extrapol: confined	1	2.1	0.29
	experi., extrapol: unconfined	1	3.3	0.19
	theory, confined	1	2.0	0.50
	theory, unconfined	1	5.6	0.18
U_p/U_w	experi., extrapol: confined	1	1.2	2.0
	experi., extrapol: unconfined	1	3.1	0.8
	theory, confined	1	2.0	0.5
	theory, unconfined	1	16	0.063

TABLE I. δ_w/δ_p and $U_p/U_w = Re_p/Re_w$ for different aspect ratios, gauged to $\Gamma = 1$, where we have put these ratios to 1. The Reynolds number $Re_p = 3.7 \cdot 10^9$ is fixed and the experimental values are extrapolated to that Re_p , see text. Note that the error in reading off in particular the boundary layer widths from the figures 3,6, and 8 of ref. [7] is at least 25% and therefore the experimental ratios should only be taken as a very rough estimate.

U_p/U_w for $\Gamma = 2$; we have no explanation for that. If extrapolated with the confined flow model both velocity ratios do not lie in between the predictions of the two flow cases.

The physics of the aspect ratio dependence is as follows: For increasing aspect ratio the available plate area of the flow increases and the plate velocity can go down. According to the Prandtl law (2), the plate BL thickness then increases. At the walls there is no additional lateral space for larger aspect ratios, therefore the flow has to accelerate, $U_w > U_p$, and correspondingly $\delta_w < \delta_p$.

Note that above dependence on Γ was derived assuming there is *one* convection roll. Once the convection develops two rolls on top of each other (for Γ less than 1) or next to each other (for Γ larger than 1), the aspect ratio dependence has to be embodied in a more sophisticated way. For small $\Gamma \leq 1/2$ a transition from one roll to two rolls has been observed numerically [18, 19]. Possibly also in experiment both states of convection have been realized, see the discussion in [8]. Thus one cannot formally consider $\Gamma \rightarrow 0$ or $\Gamma \rightarrow \infty$ in the relations (4) – (9).

Can one manipulate a system such that it is no longer in between the confined and the unconfined cases? An option may be to take a *square box* and slightly *tilt* it in order to disfavor the flow along the diagonal, which would occur without tilting [4]. If this can be achieved, one expects such flow to follow the confined flow model with confinement by the left and right walls. For this type of flow eq. (4) should hold, i.e., the wall and the plate BLs should show the same Ra -scaling. An experimental test of this predictions seems worthwhile to us to check the proposed theory.

Kinetic and thermal dissipation in the BLs: Within above framework the aspect ratio dependence can also be embodied into the unifying theory of thermal convec-

tion [11, 12]. The main idea of that theory is to split the kinetic dissipation ϵ_u and the thermal dissipation ϵ_θ , for which exact global relations can be derived from the Boussinesq equations, into their bulk and BL contributions.

For the kinetic dissipation this splitting obviously has to be extended to

$$\epsilon_u = \epsilon_{u,p} + \epsilon_{u,w} + \epsilon_{u,b}, \quad (10)$$

where $\epsilon_{u,p}$, $\epsilon_{u,w}$ mean the kinetic dissipation in the plates' or walls' BLs, and $\epsilon_{u,b}$ the bulk kinetic dissipation. Following [11], the BL dissipations are estimated as

$$\epsilon_{u,p} = \nu \frac{U_p^2}{\delta_p^2} \frac{\delta_p}{L} = \frac{\nu^3}{L^4} \frac{1}{a\Gamma^{1/2}} Re_p^{5/2} = \frac{\nu^3}{L^4} 2^5 a^{3/2} \Gamma^{-9/2} Re_w^{5/4} \quad (11)$$

and

$$\epsilon_{u,w} = \nu \frac{U_w^2}{\delta_w^2} \frac{\delta_w}{l} = \frac{\nu^3}{L^4} \frac{\Gamma^9}{2^{10} a^6} Re_p^5 = \frac{\nu^3}{L^4} \frac{1}{a\Gamma} Re_w^{5/2}. \quad (12)$$

The bulk dissipation will be dealt with below.

For the thermal dissipation the partition into BLs and bulk is different. Though at least in ideal RB convection the sidewalls are perfectly isolated (no flux condition), thermal BLs can develop at the sidewalls, as observed both in numerical simulations and in experiment [7, 19–21]. However, within our unifying theory ref. [11, 12] it is not necessary to distinguish between sidewall thermal dissipation and bulk thermal dissipation. Therefore, here we introduce the notation $\epsilon_{\theta,p}$ for the thermal dissipation in the plate BLs and $\epsilon_{\theta,\bar{p}}$ for the thermal dissipation elsewhere, i.e., within the bulk *and* within the sidewall BLs (“non-plate”).

To estimate these contributions we remind that $\epsilon_\theta = \kappa \Delta^2 L^{-2} Nu$ and that the heat current Nu consists of two terms

$$Nu = \left(\langle u_z \theta \rangle_{A,t}(z) - \kappa \partial_z \langle \theta \rangle_{A,t}(z) \right) / (\kappa \Delta L^{-1}) \\ = (\epsilon_{\theta,\bar{p}} + \epsilon_{\theta,p}) / (\kappa \Delta^2 L^{-2}) = \epsilon_\theta / (\kappa \Delta^2 L^{-2}). \quad (13)$$

Here $\langle \dots \rangle_{A,t}$ denotes the average on time and x, y -plane.

For z *outside* of the plates' thermal BLs the first term in eq. (13) dominates. We estimate $\langle u_z \theta \rangle_{A,t} \sim U \Delta$ and obtain $\epsilon_{\theta,\bar{p}} / (\kappa \Delta^2 / L^2) \sim Pr Re$. Note again that the thermal dissipation in the sidewall BLs is included in $\epsilon_{\theta,\bar{p}}$ and may even be dominant as compared to the contributions from the bulk, as the numerical simulations by Verzicco and Camussi suggest [19].

For z *within* the plates' thermal BLs, i.e., $z/L \approx 0$ or $z/L \approx 1$, the second term in eq. (13) dominates. Estimating the temperature gradient as Δ/λ_θ gives $\epsilon_{\theta,p} / (\kappa \Delta^2 / L^2) \sim L/\lambda_\theta$. To connect the BL width λ_θ with Re , we use the temperature equation $\partial_t \theta = u_j \partial_j \theta + \kappa \partial_j \partial_j \theta$, leading to $U d^{-1} \sim \kappa \lambda_\theta^{-2}$, which implies $\epsilon_{\theta,p} / (\kappa \Delta^2 / L^2) \sim \sqrt{Re Pr}$, cf. [11]. According to

this derivation the Reynolds number one has to use in $\epsilon_{\theta,\bar{p}}$ is Re_w , while $\epsilon_{\theta,p}$ is determined by Re_p .

Scaling relations for bulk velocity and temperature fluctuations: Up to now we dealt with the BLs. As for the bulk fluctuations u' , the experiments [10] suggest that they scale differently from the large scale velocity U , namely with a weaker Ra dependence. Typically, the fluctuation Reynolds number is $Re' = u'L/\nu \sim Ra^{0.40 \pm 0.03}$ and the large scale velocity Reynolds number with $Re = UL/\nu \sim Ra^{0.43 \dots 0.50}$ [3, 7, 10, 22, 23]. In refs. [11, 12] we developed a theory for the dependences $Re(Ra, Pr)$ and $Nu(Ra, Pr)$. Here we add how the fluctuations Re' and θ' should behave as functions of Ra and Pr .

The turbulence in the bulk is driven by the large scale wind, therefore $\epsilon_{u,b} \sim U^3/L$ as used in refs. [11, 12]. The energy cascades down and will be dissipated on scales comparable to the Kolmogorov scale $\eta = (\nu^3/\epsilon_{u,b})^{1/4}$. Thus we can estimate the bulk dissipation also with $\epsilon_{u,b} \sim \nu u'^2/\eta^2$. Combining both we obtain

$$Re' \sim Re^{3/4}. \quad (14)$$

With $Re \sim Ra^{0.43 \dots 0.50}$ this means $Re' \sim Ra^{0.32 \dots 0.38}$, which is close to above quoted experimental finding $Re' \sim Ra^{0.40 \pm 0.03}$ by Lam et al. [10] and also to Daya and Ecke's finding [4] $Re' \sim Ra^{0.36 \pm 0.05}$ for a square cell.

The same reasoning can be followed to calculate the scaling of the typical bulk temperature fluctuations θ' . The thermal bulk dissipation is driven by the large scale temperature Δ ; its time scale again is L/U . Thus $\epsilon_{\theta,b} \sim \Delta^2 U/L$. On the other hand, the thermal energy in the bulk is dissipated by the temperature fluctuations θ' on scale $\eta_\theta = (\kappa^3/\epsilon_{u,b})^{1/4} \sim LPr^{-3/4}Re^{-3/4}$, i.e., $\epsilon_{\theta,b} \sim \kappa \theta'^2/\eta_\theta^2$. Balancing these two expressions for $\epsilon_{\theta,b}$ one obtains

$$\theta'/\Delta \sim Pr^{-1/4}Re^{-1/4}. \quad (15)$$

With the experimental result [10] $Re \sim Ra^{0.43}Pr^{-0.76}$, which holds in $10^8 < Ra < 3 \cdot 10^{10}$ and $3 < Pr < 1200$, this means $\theta'/\Delta \sim Pr^{-0.06}Ra^{-0.11}$. For $Re \sim Ra^{1/2}$ [22, 23] one gets $\theta'/\Delta \sim Ra^{-0.13}$. Both power laws are very close to the experimental findings $\theta'/\Delta \sim Ra^{-1/7}$ [22] or $\theta'/\Delta \sim Ra^{-0.10 \pm 0.02}$ [4] for cylindrical cells.

In conclusion, we have offered a possible mechanism to cope with the recently observed effects of the RB cell geometry and the different Ra behaviors of the kinetic BLs near the plates and the sidewalls. This has to be confirmed in more experimental detail. In particular, the comparison of RB convection in a square cell with diagonal (unconfined case) and with edge parallel (confined case) wind seems promising. – Another aspect is to distinguish the 1-roll from the 2-rolls (or more) states. It seems also clear that measuring the large scale wind velocity should take notice that possibly $U_p \neq U_w$. Circulation time measurements average over both, while local methods can distinguish U_p and U_w . – Finally, we have

indicated how the global theory of Nu versus Ra, Pr has to be modified to take care of geometry effects and how the different scalings of bulk fluctuations and large scale quantities are related.

Acknowledgment: We thank X. van Doornum for drawing figure 1. The work is part of the research program of FOM, which is financially supported by NWO. It was also supported by the European Union (EU) under contract HPRN-CT-2000-00162 and by the German-Israeli Foundation (GIF).

-
- [1] L. P. Kadanoff, Phys. Today **54**, 34 (2001).
 - [2] G. Ahlers, S. Grossmann, and D. Lohse, Physik Journal **1**, 31 (2002).
 - [3] E. D. Siggia, Annu. Rev. Fluid Mech. **26**, 137 (1994).
 - [4] Z. A. Daya and R. E. Ecke, Phys. Rev. Lett. **87**, 184501 (2001).
 - [5] X. Xu, K. M. S. Bajaj, and G. Ahlers, Phys. Rev. Lett. **84**, 4357 (2000).
 - [6] G. Ahlers and X. Xu, Phys. Rev. Lett. **86**, 3320 (2001).
 - [7] X. L. Qiu and P. Tong, Phys. Rev. E **64**, 036304 (2001).
 - [8] J. Niemela and K. R. Sreenivasan, submitted to J. Fluid Mech. (2002).
 - [9] X. L. Qiu and K.-Q. Xia, Phys. Rev. E **58**, 486 (1998).
 - [10] S. Lam, X. D. Shang, S. Q. Zhou, and K. Q. Xia, Phys. Rev. E **65**, 066306 (2002).
 - [11] S. Grossmann and D. Lohse, J. Fluid. Mech. **407**, 27 (2000); Phys. Rev. Lett. **86**, 3316 (2001).
 - [12] S. Grossmann and D. Lohse, Phys. Rev. E **66**, 016305 (2002).
 - [13] L. Prandtl, *Verhandlungen des III. Int. Math. Kongr., Heidelberg, 1904* (Teubner, Leipzig, 1904), page 484.
 - [14] H. Blasius, Z. Math. Phys. **56**, 1 (1908).
 - [15] L. D. Landau and E. M. Lifshitz, *Fluid Mechanics* (Pergamon Press, Oxford, 1987).
 - [16] This follows from applying Pythagoras' theorem to figure 1a, bottom, and holds for small $\delta_w \ll d$.
 - [17] Note that it is the *plate* Reynolds number Re_p which is measured in ref. [7] where it is called Re_γ . It is extracted from the slope of the (linear) profile of the horizontal velocity above the bottom plate.
 - [18] J. Werne, Phys. Rev. E **48**, 1020 (1993).
 - [19] R. Verzicco and R. Camussi, submitted to J. Fluid Mech. (2002).
 - [20] G. Ahlers, Phys. Rev. E **63**, 015303 (2000).
 - [21] E. S. C. Ching and K. F. Lo, Phys. Rev. E **64**, 046302 (2001); E. S. C. Ching and K. M. Pang, Eur. Phys. J. B **27**, 559 (2002).
 - [22] B. Castaing *et al.*, J. Fluid Mech. **204**, 1 (1989).
 - [23] J. Niemela, L. Skrebek, K. R. Sreenivasan, and R. J. Donnelly, J. Fluid Mech. **449**, 169 (2001).